Auger effect in the Mn^{2+} luminescence of CdF_2:(Mn,Y) crystals

Andrzej Suchocki and Jerzy M. Langer
Institute of Physics, Polish Academy of Sciences, Aleja Lotników 32/46, PL-02-668 Warszawa, Poland
(Received 6 July 1988)

The energy transfer between the Mn^{2+} ions and free electrons and electrons bound on shallow donors in CdF_2:Mn,Y crystals has been examined. This so-called Auger effect on localized impurities turned out to be a very efficient quenching mechanism of the deep luminescent centers in semiconductors. Experimental evidence for such an effect is presented. It is proved that the dipole-dipole mechanism of the energy transfer is responsible for the luminescence quenching due to the free electrons unlike the quenching due to the weakly bound electrons where the exchange mechanism causes the decrease of the luminescence quantum efficiency. The theory presented here explains the experimental results very well. The Auger effect due to the free electrons is important at higher temperatures and was proved to be about 500 times more efficient than the Auger effect due to the shallow donors, which is important only at low temperatures. There are also arguments presented explaining problems with the designing of the dc-mode injection-type laser diodes based upon the intraimpurity emission.

I. INTRODUCTION

The mechanism of the nonradiative recombination of the excited states of impurities in insulating crystals and semiconductors has long been a topic of fundamental interest in solid-state physics.[1-4] It has been found that multiphonon processes usually dominate nonradiative recombination for localized defects.[1-3] The probability of these processes is dependent on the type of coupling with lattice vibrations. For weakly coupled defects the nonradative deexcitation rate depends exponentially on the energy ΔE to be dissipated. This dependence is known as the "energy-gap law"[3] and its validity has been verified for rare-earth impurities in a variety of hosts. In strongly coupled systems the nonradiative recombination is generally a thermally activated process, since it proceeds via the energy barrier at the crossing of the two levels.[3-5] If the energy ΔE is high compared with the highest energy of phonons in the host or the temperature is sufficiently low, the probability of the multiphonon nonradiative recombination becomes small and other types of recombination become more competitive. One of them is energy migration through the system of excited ions and energy transfer to different types of defects, where the excitation energy can be dissipated easier.[2,4,6] All these nonradiative processes have been most extensively studied in insulating crystals.

In semiconductors, the presence of carriers (free or weakly bound on shallow donors or acceptors) opens a new recombination channel—the Auger effect (AE).[1,7] In contrast to those already discussed, the energy acceptor in this case is either the free carrier or the carrier bound to some defect center. In any case the energy accepting carrier is promoted during the AE high into the respective band (the conduction band for the electrons and valence band for the holes). The AE involving either free or weakly bound carriers was proved to be responsible for the luminescence quenching for various types of bound excitons or donor-acceptor pairs[8] but it was commonly neglected as an efficient nonradiative deexcitation mechanism of localized centers in semiconductors. In 1981 Gordon and Allen[9] in ZnS:Mn^{2+} and our group[10,11] in CdF_2:Mn^{2+} have independently found that the intrashell Mn^{2+} luminescence is very efficiently quenched in conducting crystals. The efficiency of this mechanism has been confirmed in the intrashell luminescence quenching of several rare-earth dopants in semiconductors[12] as well as in case of Fe in ZnS and InP.[13] The magnitude of the intrashell luminescence quenching by the AE is in most cases well reproduced by the theoretical estimations made by one of us.[14] The reasons for the surprisingly large efficiency of the AE will be discussed in more detail in the next sections.

In contrast to the free-carrier AE, the AE due to energy transfer to weakly bound carriers has been found to be much weaker. It can be observed only at low temperatures at which the carriers freeze out on shallow donors. Until now the only unambiguous case of this type of the AE has been found in the luminescence of Mn^{2+} in conducting CdF_2.

It is the main purpose of this paper to provide a complete experimental and theoretical analysis of both types of the AE at localized centers in semiconductors. The experimental observations shall be reported for the intraimpurity $Mn^{2+}(3d^5)$ emission in conducting CdF_2 crystals.

CdF_2 crystals, unlike other fluorities, can be converted to the conductivity state by doping and appropriate annealing with most trivalent impurities.[15-17] The annealing process causes a diffusion of the interstitial fluorines acting as the deep acceptors compensating the extra charge of the trivalent dopants.[15] It is possible to control the electron concentration by the doping level and annealing conditions up to about 4×10^{18} cm^{-3} at room temperature.[16] CdF_2 crystals doped with rare-earth or manganese ions can also be a source of efficient photoluminescence or electroluminescence but the photo-

luminescent properties disappear rapidly with an increase of the electron concentration.

The two paths of the energy transfer from the excited Mn^{2+} ions, one to the free electrons and the second to the electrons bound at the shallow donors (Fig. 1) are responsible for the luminescence quenching. The existence of both types of the AE manifests itself in the temperature dependence of the quantum efficiency of the CdF_2:Mn,Y crystals, highly converted to the conductivity state (Fig. 2). At temperatures above 100 K, the characteristic intrashell ($^4T_{1g} \rightarrow {}^6A_{1g}$) manganese luminescence[18] is practically completely quenched. For temperatures below 100 K, i.e., in the temperature range in which the carrier concentration decreases strongly, the luminescence becomes visible. At the lowest temperatures (below 40 K), when practically all electrons are frozen out at the shallow donors,[16] the luminescence quantum efficiency reaches its maximum. Its magnitude, as we shall show later, depends on the concentration of the occupied shallow donors. This experiment provides that the AE due to electrons bound at shallow donors is responsible for the decreasing of the luminescence quantum yield in this temperature region, while at higher temperature the free-carrier AE dominates.[19]

Independent evidence of the intrashell Mn^{2+} luminescence quenching by the AE is given by the observation of the reverse-bias dependence of the Mn^{2+} cathodoluminescence generated under a thin gold gate evaporated on a semiconducting CdF_2:Mn crystal[11,20,21] (no cathodoluminescence is observed in this crystal if excited directly, i.e., not through the metal gate). The increase of the reverse bias (still much below the onset of the electroluminescence in this structure) causes the increase of the intensity of the cathodoluminescence (Fig. 3). This increase is proportional to the volume of the electron-depleted region beneath the metal gate forming a Schottky barrier on the surface of the CdF_2 substrate. Since the penetration depth of the injected electrons is much larger than the depletion layer width, Mn excitation can be assumed to be spatially uniform. The depletion layer beneath the metal gate is equivalent to the insulating crystal, i.e., the region where there is no AE due to either free or weakly bound electrons. The increase of the reverse bias causes the increase of the electron-free volume and thus the increase of the AE free region. This is the reason for a linearity of a total Mn^{2+} emission versus the depletion layer width. This experiment explains why a very efficient electroluminescence can be achieved in the metal-semiconductor (MS) or metal-insulator-semiconductor (MIS) structures made on semiconducting CdF_2 substrates doped with one of the luminescence activators (Mn or rare-earths ions).[20] There the luminescence is generated in the depletion layer, where the electron concentration is very small and therefore this layer is equivalent to the insulating crystal. Thus it is possible to observe very efficient electroluminescence from the MS or MIS structures on *conducting* CdF_2 crystals containing different luminescent impurities,[11,21] the crystals being very poor luminophors if excited by light.

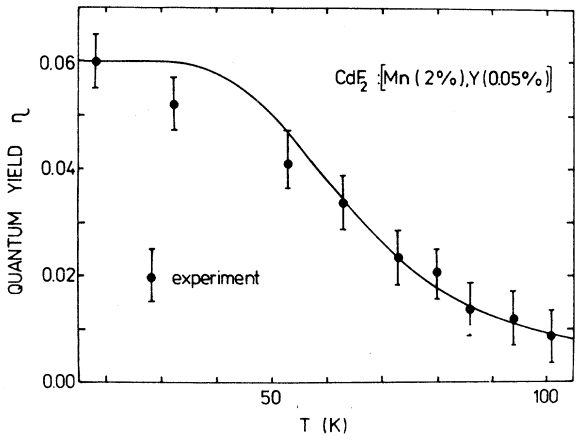

FIG. 2. The temperature dependence of the luminescence quantum efficiency of strongly conducting CdF_2:Mn(2 mol %), Y(0.05 mol %) crystals. The solid line is a fit to equation: $\eta=[1/\eta_0+A\exp(-\Delta E/kT)]^{-1}$. Here the exponential factor reflects such a temperature dependence of the electron concentration.

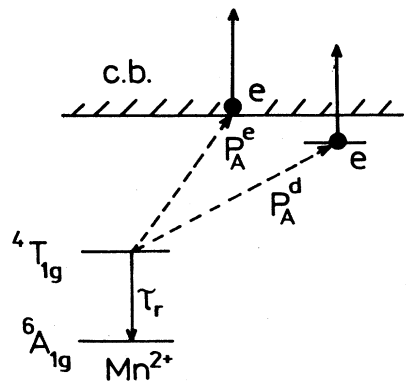

FIG. 1. The two kinds of the localized-center Auger effect in conducting crystals. Manganese is taken here as an example of the localized impurity.

The major part of this paper is devoted to the characterization of the energy-transfer mechanism which is responsible for the existence of both types of the AE. Unambiguous verification of the energy-transfer mechanism is not an easy task. We show that the simple dipole-dipole mechanism suffices to explain the strength of the AE due to free electrons. In contrast to it, the manganese luminescence quenching by electrons weakly bound at shallow donors at low temperatures is governed by the exchange interaction, which is well explained by the theory presented here.

II. SAMPLES AND EXPERIMENTAL TECHNIQUES

The crystals used in our experiments (doped with Mn 1 mol % and doubly doped with 1% or 2% of Mn and 0.05% mol % of Y) were grown by a Bridgeman-

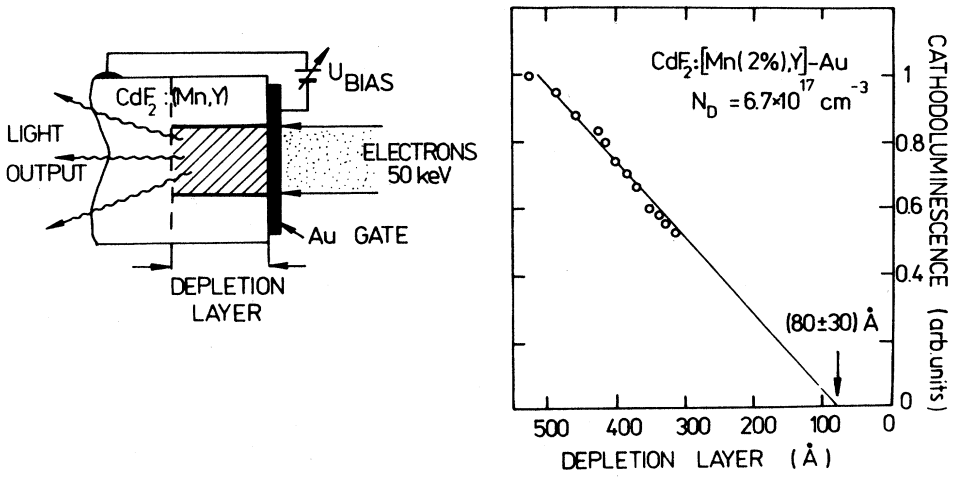

FIG. 3. Cathodoluminescence of a CdF_2:Mn,Y-Au Schottky diode vs the width of the depletion layer.

Stockbarger method from powdered CdF_2 purified by several zone melting runs and mixed with appropriate amounts of MnF_2 and YF_3. The cylindrical crystals about 1 cm in diameter were cut and mechanically polished on a diamond paste. Conversion to the conductivity state of the crystal samples has been done by the annealing in an H_2 atmosphere at temperatures between 130 and 500 °C for a few minutes up to 1.5 h depending on the desired level of conversion. This type of annealing process is believed to remove the interstitial compensating fluorine ions from the crystal.[15] This causes liberation at the surface of the free electrons trapped further by the shallow Y donors. After annealing the samples were repolished.

As a result of the annealing process, the neutral shallow donors are formed. Their activation energy depends on their concentration and reaches the limit of 110 meV for very weakly doped samples.[16,22] The high-energy tail of the shallow hydrogeniclike donor photoionization absorption,[17] extending up to the visible region, causes a blue color in more heavily converted samples.

The absorption spectra were measured in a Hitachi-Perkin Elmer model 340 uv-visible spectrophotometer in the visible and near-infrared (ir) range, while the infrared absorption spectra of the shallow donors were measured using a Carl Zeiss Specord model 71 ir spectrophotometer. The excitation spectra of the luminescence were taken using a xenon lamp as a light source and a SPM-2 Carl Zeiss monochromator. The spectra were corrected for different penetration depths for the light in the regions of very high absorption near the band gap of CdF_2. The luminescence was excited by the 457.0-nm line of a Carl Zeiss ILA 120 argon-ion laser and the 337.1-nm line of a pulsed nitrogen laser. Both types of excitation are intrashell.[18] The luminescence spectra were analyzed by a GDM-1000 double-grating monochromator with a Hamamatsu type 666 photomultiplier and an ITHACO 393 lock-in amplifier. The decay kinetics were stored in a model 4202 EG&G PAR Signal Averager and processed by a computer.

III. LUMINESCENCE OF Mn IN INSULATING CdF_2 CRYSTALS

$Mn^{2+}(3d^5)$ in CdF_2 is a very efficient activator of a blue-green luminescence.[18–20] The luminescence spectrum of insulating CdF_2:Mn(1 mol %) crystal is shown in Fig. 4. The luminescence can be excited either via a coactivator (e.g., oxygen or interstitial fluorine ions) or through the intrashell excitation.[18] There is one broad band with no fine structure which corresponds to transitions from the first excited state $^4T_{1g}(^4G)$ to the $^6A_{1g}(^6S)$ ground state of the Mn^{2+} ion in a centrosymmetric environment.[18]

The excitation of Mn^{2+} luminescence and the absorption spectra of CdF_2:Mn are presented in Fig. 5. The spectra consist of several bands placed between 500 and 300 nm corresponding to the intrashell (d^5) transitions from the ground state to the subsequent excited states. The assignment of the bands to the crystal-field states of the Mn^{2+} ion in an O_h environment is also shown in Fig. 5. The last broad band peaked about 260 nm is most probably caused by the absorption of O^{2-} ions followed by energy transfer to the Mn^{2+} ions.[18,23] The intrashell Mn^{2+} transitions are also observed in the absorption measurements. The intrashell transitions are highly spin and symmetry forbidden and therefore their oscillator strengths are very low (in the range of 10^{-8}), much less than in other crystals doped with Mn (e.g., in ZnS). The absorption spectrum correlates very well with the excitation spectrum, excluding only the band around 260 nm, observed in the excitation measurements. This band is difficult to observe in the absorption measurements since it is overlapped with the band-edge absorption.

The temperature dependence of the luminescence decay kinetics of CdF_2:Mn (1 mol %) is shown in Fig. 6. The decay kinetics are exponential for all measured temperatures between 4.2 and 400 K. The decay time of the luminescence is equal to 156±3 ms at $T=10$ K and diminishes slowly to about 60 ms at $T=320$ K. Vibronic processes are responsible for this decrease. An additional

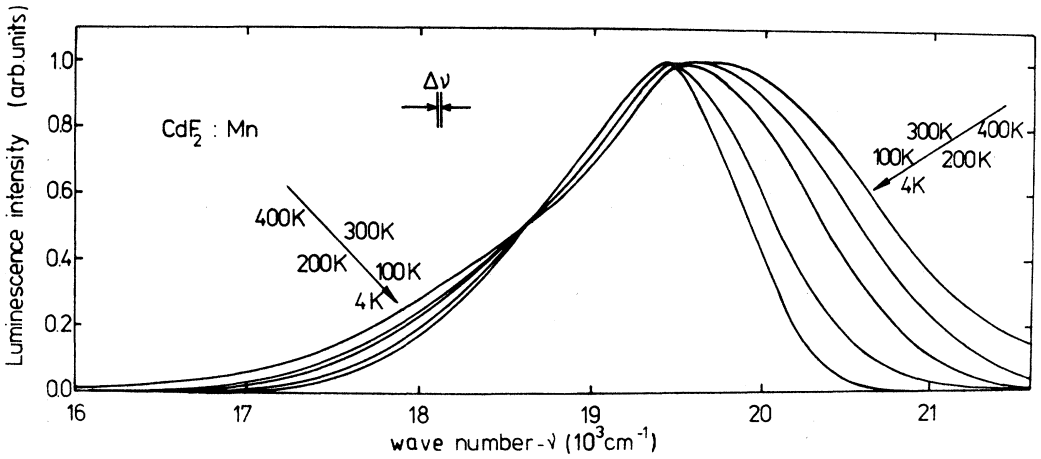

FIG. 4. The luminescence spectra of insulating CdF_2:Mn(1 mol %) at different temperatures.

fast decrease of the decay time is observed above 320 K and it is associated with nonradiative deexcitation processes.

The radiative decay time of the luminescence τ_r are related to the oscillator strength f_0 of the transition by the expression (for electric-dipole transitions):[24]

$$\tau_0 f_0 = \frac{1.5}{n_r^2} \frac{\tilde{\nu}_{\text{abs}}}{\tilde{\nu}_{\text{em}}^3} \frac{g_e}{g_f} , \tag{1}$$

where n is the refractive index of the crystal, $\tilde{\nu}_{\text{abs}}$ and $\tilde{\nu}_{\text{em}}$ are the wave numbers for absorption and emission, and g_e and g_f are the degeneracies of the excited ($^4T_{1g}$) and the ground ($^6A_{1g}$) states, respectively. Substituting into this equation the results of the absorption measurements for the $^6A_{1g}(^6S) \rightarrow {}^4T_{1g}(^4G)$ transition (oscillator strength $f_0 = [(2.5 \pm 0.4) \times 10^{-8}$ at $T = 10$ K] we obtain a value of τ_r equal to 153 ± 25 ms which is in very good agreement with that observed. The product of the luminescence decay time and the oscillator strength is constant up to about 320 K (Fig. 7), which means that the quantum efficiency of these transitions is close to unity below 320 K.

Clustering effects of the Mn^{2+} ions can be observed for higher manganese concentrations,[18] e.g., the shift of the luminescence spectrum towards lower energies, existence of additional lines in the low-temperature absorption, and excitation spectra, strong nonexponentiality of the luminescence decay kinetics, and finally above 5% of Mn concentration quenching occurs. No such effects of the

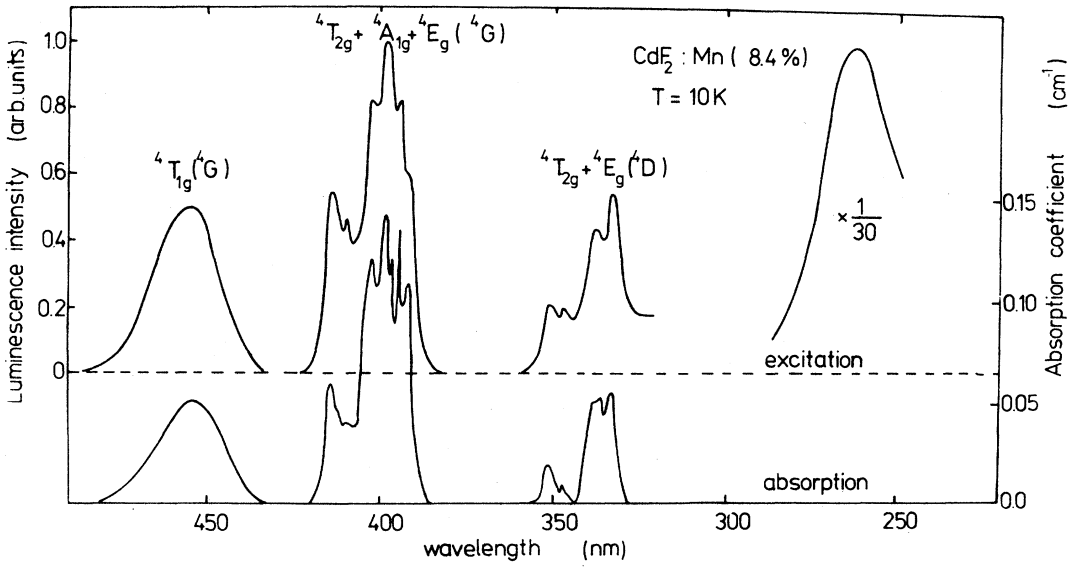

FIG. 5. The absorption and excitation of the Mn^{2+} luminescence spectra in CdF_2:Mn(8.4 mol %) crystal at $T = 10$ K.

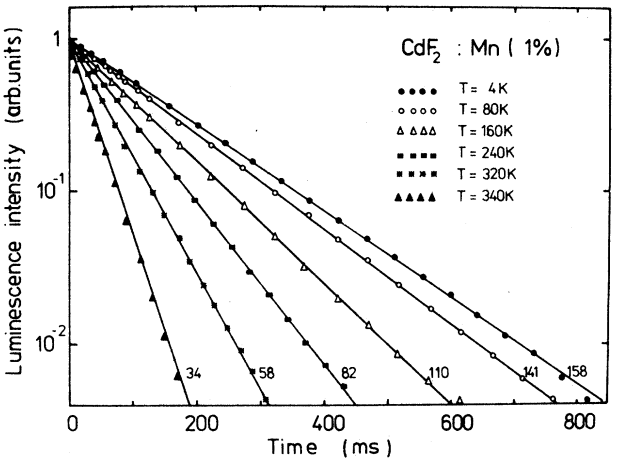

FIG. 6. The temperature dependence of CdF_2:Mn^{2+} luminescence decay kinetics. Lifetime values are given units of ms.

manganese luminescence have been observed in the samples used for the study of the Auger effect since manganese concentration in these samples did not exceed 2 mol %.

IV. Mn LUMINESCENCE QUENCHING BY THE FREE-ELECTRON AUGER EFFECT

A. Experimental results

Highly conducting CdF_2:Mn crystals do not luminesce at room temperature. The characteristic

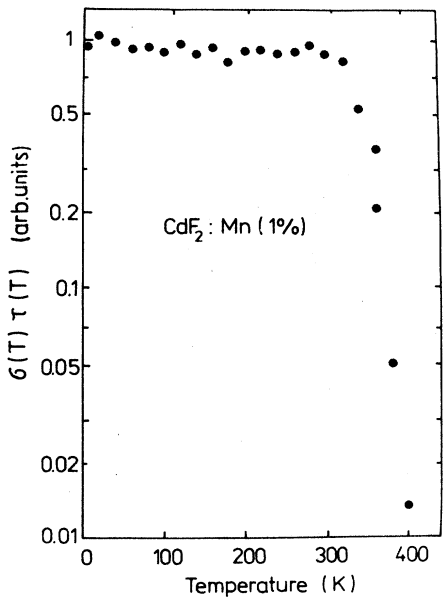

FIG. 7. The temperature dependence of the normalized product of the Mn^{2+} luminescence decay time and the oscillator strength of the ${}^4T_{1g}({}^4G) \rightarrow {}^6A_{1g}({}^6S)$ transitions for the CdF_2:Mn (1 mol %) crystal.

$Mn^{2+}({}^4T_{1g} \rightarrow {}^6A_{1g})$ green luminescence can be seen in these crystals only upon cooling (Fig. 2). This luminescence can be seen at room temperature only in crystals at which the room temperature free-electron concentration does not exceed 10^{17} cm^{-3}. The probability of the intraimpurity luminescence quenching by the free-electron AE should be *linear* in the free-carrier concentration:

$$P_A = C_A n \ . \tag{2}$$

Such a relationship if experimentally observed, serves as the best evidence of this mechanism. From the preceding remarks it is clear that the necessary range of carrier concentration is below 10^{17} cm^{-3}. There are three ways to achieve this goal. One is a suitably low doping. In CdF_2 the thermal ionization energy of shallow donors depends on their concentration[16,22] and reaches a limit of about 100 meV for a vanishing doping level. This means a donor doping level not exceeding 10^{17} cm^{-3} (about 10 ppm). This level is unfortunately at the limit of the present state of the art in growth technology of weakly compensated CdF_2. An alternative way of obtaining this range of donor concentration is only a partial deconversion of doubly doped CdF_2:Mn,Y crystal by a proper annealing (either very short annealing time in an H_2 stream or Cd vapors at $T_a \approx 500\,°C$ or longer annealing at lower temperatures). In any case the degree of compensation remains close to unity, which generally results in a nonunformity in the carrier concentration. The third way to achieve the required carrier concentration is a crystal cooling which causes freezeout of the free carriers on the shallow donors. This procedure can be used on totally converted samples and thus guarantees, in principle, the highest carrier uniformity in the crystal.

The typical temperature dependence of the luminescence quantum efficiency of the *highly converted* CdF_2:Mn(2 mol. %),Y crystal with the shallow donor concentration of about $N_D(Y) = 1.3 \times 10^{19}$ cm^{-3} is shown in Fig. 2. The measurements were taken by comparison of the luminescence intensity of this crystal with the luminescence intensity of the identical slab of an insulating one. The comparison is equivalent to the measurement of the luminescence quantum efficiency since at temperatures below 300 K the luminescence quantum yield of the insulating crystal is close to 100%. Because the free-electron AE is proportional to the free-electron concentration [Eq. (2)], the luminescence quantum efficiency of the crystal is therefore equal to

$$\frac{1}{\eta} = \frac{1}{\eta_0} + C_A \tau_r n = \frac{1}{\eta_0} + \frac{n}{n_0}, \quad n_0 = (C_A \tau_r)^{-1} \ , \tag{3}$$

where $\eta(T)$ is a total emission efficiency, η_0 is the emission efficiency of the insulating crystal, and the n_0 is the critical carrier concentration at which the radiative and the Auger quenching probabilities are equal.

Figure 8 shows the temperature dependence of the additional nonradiative decay probability as derived from the emission efficiency data shown in Fig. 2 The dependence of the free-electron concentration on temperature, calculated from the resistivity of the sample measured by a four-probe method,[23] assuming a temperature-

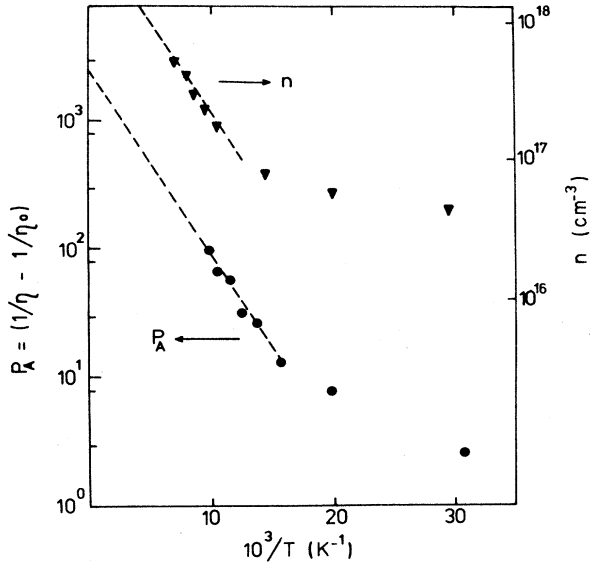

FIG. 8. The temperature dependence of the Auger quenching P_A of the CdF_2:Mn(2 mol %),Y(0.05 mol %) crystal, ● and free-carrier concentration n, ▼.

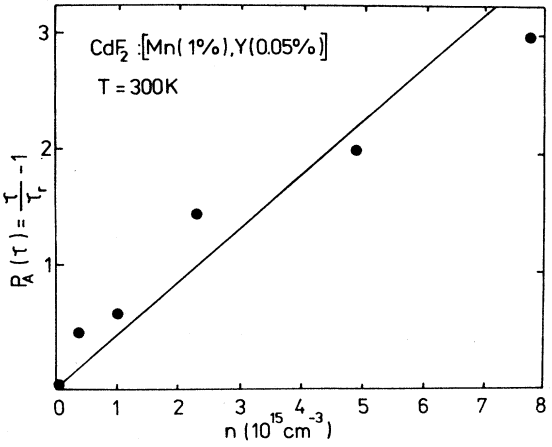

FIG. 9. The probability of the Auger effect P_A calculated from the luminescence decay kinetics.

independent electron mobility $\mu_{el}=5$ cm^2/V s (Ref. 16) is also shown in Fig. 8. It is evident from the data in Fig. 8 that the additional quenching correlates well with the free-electron concentration at higher temperatures. At lower temperatures the accuracy of the resistivity measurement is rather poor because of the very high resistivity of the crystal. From the results of the Fig. 8 the critical concentration n_0 is equal to $n_0=2\times10^{15}$ cm^{-3}.

In order to verify this result we have performed efficiency and kinetics measurements at room temperature on the *weakly converted* CdF_2:Mn(1 mol %),Y samples with different carrier concentrations at room temperature. The decay kinetics, excited by the nitrogen laser, are strongly nonexponential. This indicates nonuniformity of the free-electron concentration in the sample. The decay times used to estimate the AE strength were calculated from the exponential tails of the decay kinetics to avoid the possibility that the shortening of the lifetimes might be connected with an effect other than the increase of the free-electron concentration. The dependence of the Mn^{2+} lifetimes on the free-electron concentration at room temperature is shown in Fig. 9. The critical concentration n_0 calculated from this results is equal to $n_0=2.2\times10^{15}$ cm^{-3}, which is in excellent agreement with the previous result.

The probability P_A of the AE due to free electrons calculated from the Mn^{2+} luminescence quantum yield is also linear with respect to the free-electron concentration and therefore correlates well with the luminescence kinetics measurements. Nevertheless the critical concentration n_0 obtained from these measurements is smaller than calculated from the previous experiments which is most probably caused by the nonuniform distribution of the uncompensated donors in these very weakly converted samples.

B. Theory

The free-electron AE rate C_A is calculated in the standard perturbation manner, i.e.,

$$C_A=\frac{2\pi}{\hbar}\frac{g_0}{g_e}\frac{1}{8\pi^3}\int_{BZ}d^3k\,M^2(\mathbf{k})\delta(E(\mathbf{k})-E_0)\ , \qquad (4)$$

where E_0 is the quenched emission energy, g_0 and g_e are the degeneracies of the ground and excited states of the quenched center, BZ denotes the Brillouin zone, and the integration is carried out over all the free-electron states conserving energy. These are characterized by the crystal wave vector $\mathbf{k}$ and dispersion energy law $E(\mathbf{k})$.

The wave functions of the interacting system can be written as Slater determinants composed of the quenched center wave functions $\Psi(\mathbf{R})$ and the electron (or hole) in the conduction (or valence) band:

$$\begin{aligned}&\Phi_i=|\Psi_e(\mathbf{R})u_0(\mathbf{r})|,\quad E_i=E_0=h\nu\\&\Phi_f=|\Psi_0(\mathbf{R})u_k(\mathbf{r})e^{i\mathbf{k}\cdot\mathbf{r}}|,\quad E_f=E(\mathbf{k})\ .\end{aligned} \qquad (5)$$

Here, $u_0(\mathbf{r})$ and $u_k(\mathbf{r})$ are the strongly oscillating periodic parts of the Bloch wave functions at the bottom of the conduction (top of the valence) band and at the energy $E(\mathbf{k})$. The interaction between all these electrons is simple Coulombic.

The $\mathbf{k}$-dependent matrix element is the difference between the Coulomb and the exchange terms:

$$M^2(\mathbf{k})=|M_c(\mathbf{k})-M_{EX}(\mathbf{k})|^2\ . \qquad (6)$$

Since the final states belong to the crystal band continuum, the resonance condition is always fulfilled. To estimate the lower limit of the C_A it is enough to compute the Coulomb term only. Due to the localized nature of the emitting center the Coulomb interaction can be expanded into the multipole series. The first term leads to a

dipole-dipole interaction. To give the lower boundary of the AE probability C_A, calculation of this term suffices. It equals

$$M_c^d = \frac{e^2}{\varepsilon(E_0)} \left[\frac{\varepsilon_{\text{eff}}}{\varepsilon_0} \right] \left\langle \Phi_i \left| \frac{\mathbf{r}\cdot\mathbf{R}}{r^3} \right| \Phi_f \right\rangle . \quad (7)$$

Here the crystal-field correction has been included. The way this correction was incorporated follows the arguments of Agranovich[26] on the screening of the dipole-dipole interaction in the case of localized centers. The dielectric function at energy E_0 can reasonably be approximated by the high-frequency dielectric constant $\epsilon_\infty = n_r^2$ (n_r is the refractive index at the energy E_0). Substituting into Eq. (7) the system wave functions lead to separation of the matrix element M_c^d into the product of the optical electric-dipole matrix element for a localized center $|\langle \Psi_e|\mathbf{R}|\Psi_0\rangle|^2$ and a function dependent only on the band electron $\mathbf{k}$ vector. The electric-dipole matrix element is related to the electric-dipole radiative lifetime τ_r^{ED}:

$$\frac{g_0}{g_e}|\langle \Psi_e|\mathbf{R}|\Psi_0\rangle|^2 = \frac{3}{4}\frac{1}{n_r}\left[\frac{\varepsilon_0}{\varepsilon_{\text{eff}}}\right]^2 \frac{\hbar^4 c^3}{e^2 E_0^3}\frac{1}{\tau_r^{\text{ED}}} . \quad (8)$$

Substituting this result into Eq. (7) and then into Eq. (4) we recover the postulated form of C_A [Eq. (2)], namely, its proportionality to the quenched center radiative probability ($P_r = 1/\tau_r$):

$$C_A = \frac{1}{\tau_r}\frac{1}{n_0} , \quad (9)$$

where the critical carrier concentration n_0 depends only on the parameters of the crystal and not on the details of the localized-center wave function. It is equal to

$$n_0 = \frac{2k_0^2}{e^2} n_r^5 \frac{1}{|F_c|^2} \lambda_0^{-3} \mathcal{N}_c^{-1}(E_0) , \quad (10)$$

where $F_c = \langle u_c(\mathbf{r})|u_k(\mathbf{r})\rangle$, k_0 corresponds to the Brillouin-zone region contributing mainly to the density of states $\mathcal{N}_c^{-1}(E_0)$ (usually the edge), and λ_0 is the emission wavelength. From this equation the enhancement of the AE by the high density of band states is evident. This equation can be simplified further by employing the parabolic approximation, i.e., assuming that $E(\mathbf{k}) = \hbar^2 k^2/2m^*$ and assuming a value of unity for F_c (the exact values of F_c are very close to this value). In this approximation

$$n_0 = 4\pi^{5/2} n_r^5 \left[\frac{m_0}{m^*} 137 a_0\right]^{1/2} \lambda_0^{-7/2} , \quad (11)$$

where a is the Bohr radius ($a = 0.53$ Å). Substituting characteristic parameters for CdF_2:Mn emission ($\lambda_0 = 0.52$ μm, $n_r = 1.57$) and putting m^*/m_0 ratio equal unity we obtain the theoretical value of $n_0 = 6\times 10^{14}$ cm^{-3}. The $k=0$ value of the m_e^*/m_0 for CdF_2 is close to 0.4 without taking into account the polaron enhancement of this value. Since the final state of the Auger particle is very high in the conduction band, taking $m^* \approx m_0$ seems to be the best solution. The good agreement between the experimental value of n_0 and that calculated above should be taken only as an indication of the possibility of a large contribution of the dipole-dipole term in the expansion of the Coulomb interaction in the multipolar series. Although the contribution of the next term is unlikely to be so large, the exchange interaction may be, as it will be shown later, of the same order of magnitude. In the case of the AE due to shallow donors the latter contribution governs the Auger quenching.

V. Mn LUMINESCENCE QUENCHING BY THE AUGER EFFECT DUE TO ELECTRONS BOUND ON SHALLOW DONORS

A. Experimental results

This kind of AE resembles the well-known case of resonant energy transfer between localized centers, which was examined by many authors, beginning from Forster[27] and Dexter.[28] The key difference is that the final state of the quencher is not its localized discrete state but the ionized state with the electron excited high into the conduction band. In order for such transfer to be possible the luminescence spectrum of the sensitizer ions (in our case the Mn^{2+} ions) must overlap the absorption spectrum of the activator ions (in our case the photoionization spectrum of the shallow donors). Because of the continuous character of the photoionization spectrum of the shallow Y donors (Fig. 10) this resonance condition is always fulfilled. To eliminate the free-electron AE cooling of the CdF_2:Mn,Y crystals down to liquid-helium temperature was employed. At this temperature all electrons are frozen out on shallow donors. The AE due to electrons bound on shallow donors requires much more elaborate analysis in comparison with the free-electron AE due to the spatial dependence of the energy-transfer probability in this case. This leads to nonexponential kinetics of the luminescence decays clearly seen in Fig. 11. These kinetics were measured at 4.2 K after pulsed excitation by the 337.1-nm line from the nitrogen laser.

The exact dependence of the energy-transfer rate on the distance R between the excited Mn^{2+} ions and the occupied shallow donors depends on the detail mechanism of the energy transfer. If one of the multipolar mechanisms dominates, the distance dependence is[28]

$$P_A = \frac{1}{\tau_r}\left[\frac{R_0}{R}\right]^m , \quad (12)$$

where R_0 is the critical distance at which the AE rate equals the radiative probability and $m=6$ for electric dipole-dipole transfer (higher values of m are expected for the higher multipolar interactions[28]). In the case where the exchange mechanism dominates, the transfer rate depends exponentially on the distance, as we shall prove later.

In any case, assuming a statistical distribution of the sensitizer and activator ions, lack of energy migration through the system of excited ions and isotropic properties of the energy transfer the luminescence intensity $I_i(t)$

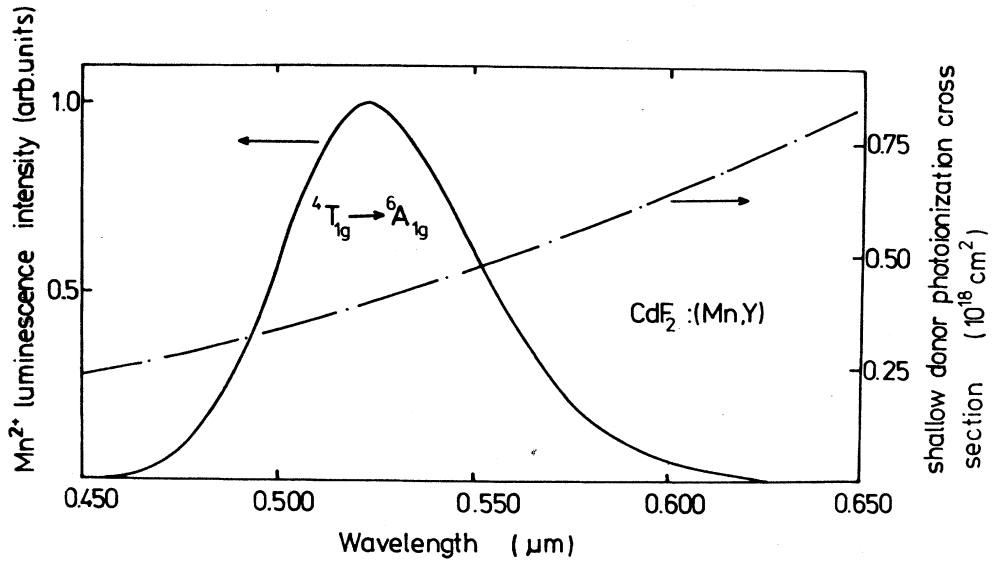

FIG. 10. The spectrum of the Mn^{2+} photoluminescence and the shallow donor photoionization cross section of the CdF_2:Mn,Y crystals.

of the sensitizer ions at time t after an excitation pulse can be written as the following product[29]:

$$I_i(t)=I_0\exp\left[-\frac{t}{\tau_r}\right]\exp\left[-\frac{C}{C_0}f_i\left[\frac{t}{\tau_r}\right]\right], \tag{13}$$

where τ_r is the radiative lifetime of sensitizer ions, C—activator concentration, $C_0=3/(4\pi R_0^3)$ and f_i is a universal function dependent only on the kind of interaction. For an electric multipole interaction f_i is equal to[29]:

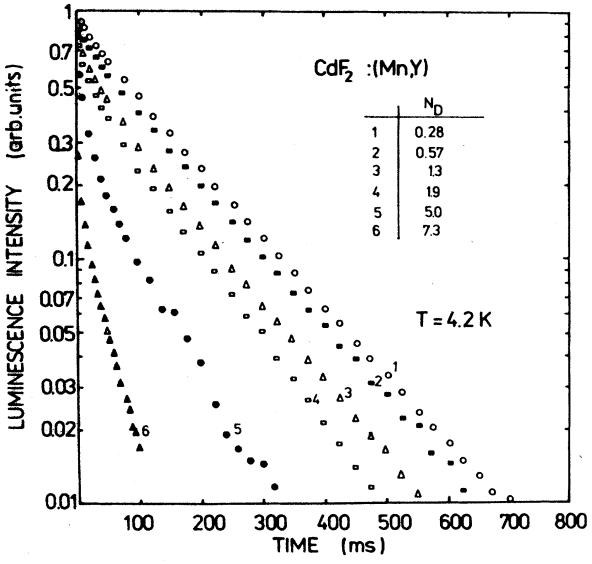

FIG. 11. The normalized photoluminescence decay kinetics of the CdF_2:Mn(1 mol %),Y(0.05 mol %) crystals at $T=4.2$ K vs shallow donor concentration. The shallow donor concentrations N_D are given in 10^{18} cm^{-3} units.

$$f_m=\Gamma(1-3/m)\left[\frac{t}{\tau_r}\right]^{3/m}, \tag{14}$$

where $m=6,8,10$ for the electric dipole-dipole (EDD), electric dipole-quadrupole (EDQ), etc., type of interaction, respectively, and $\Gamma(x)$ is the γ function. For exchange (EX) interaction[29]

$$f_{EX}=\gamma^{-3}g\left[\frac{e^{\gamma}t}{\tau_r}\right], \tag{15}$$

where $\gamma=(2R_0)/a_B$, and a_B is the Bohr radius of the center characterized by a more diffused wave function (in our case—the shallow donor), and

$$g(x)=6x\sum_{m=0}^{\infty}\frac{(-x)^m}{m!(m+1)^4}. \tag{16}$$

Figure 12 shows the $f_i(t/\tau_r)$ functions for several possible energy-transfer mechanisms versus $(t/\tau_r)^{1/2}$ for the same C/C_0 value. The f_i for the dipole-dipole mechanism is a straight line on this scale. Since the value of τ_r is known for Mn^{2+} it is convenient to make a correlation plot between the theoretical function f_i for several mechanisms and a modified experimental kinetic in the form[30]

$$f^*\left[\frac{t}{\tau_r}\right]=-\ln\left[\frac{I\left[\frac{t}{\tau_r}\right]}{I_0}\exp\left[\frac{t}{\tau_r}\right]\right]. \tag{17}$$

Plotting the modified experimental kinetics $f^*(t/\tau_r)$ versus the theoretical $f_i(t/\tau_r)$ for each quenching mechanism (an example of such a plot is presented in Fig. 13) allows for the determination of the C/C_0 ratio (Table I). From our experience the above-mentioned fits do not strongly discriminate the transfer mechanism, even if the

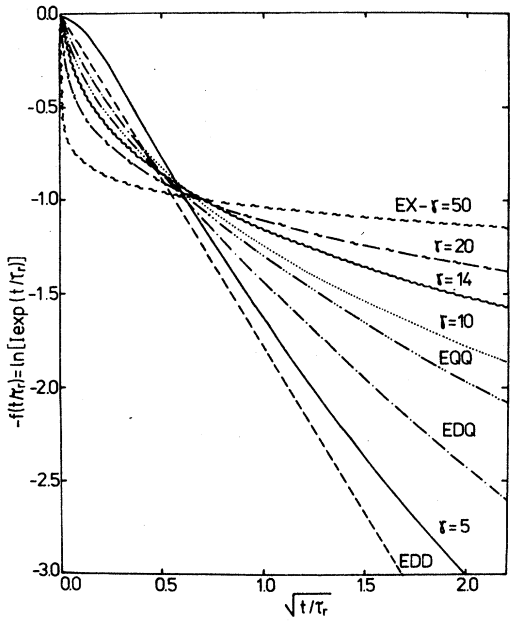

FIG. 12. The modified theoretical sensitizer luminescence decay kinetics for various types of dominant energy-transfer interaction mechanisms.

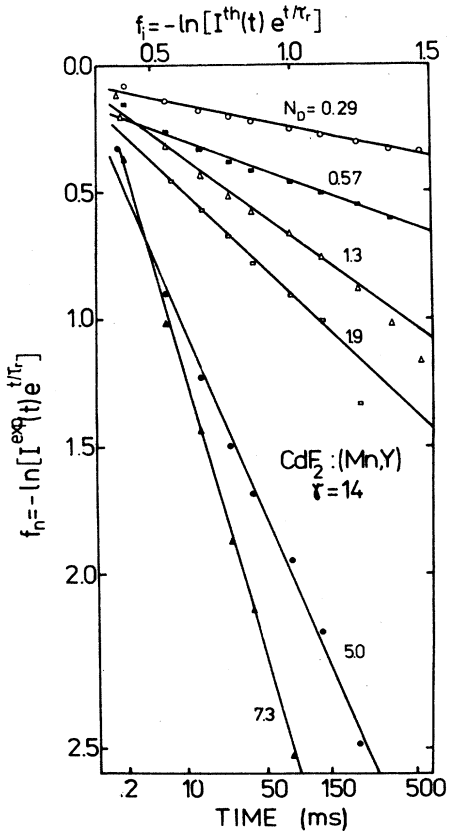

FIG. 13. Correlation kinetics diagram for exchange interaction with parameter $\gamma=14$.

TABLE I. The concentration of shallow donors C_0, the critical radius R_0, the shallow donor Bohr radius, and the critical concentration of the free electrons for different types of interaction calculated from the results of the luminescence quenching experiments of CdF_2:Mn due to the Auger effect on electrons bound on shallow donors.

	C_0 (10^{18} cm^{-3})	R_0 (Å)	L (Å)	n_0 (EX) (cm^{-3})
EDD $m=6$	4.6	37		
EDQ $m=8$	3.1	42		
EQQ $m=10$	2.6	45		
EX $\gamma=10$	2.7	45	9.0	2.0×10^{16}
EX $\gamma=14$	1.9	50	7.2	7.2×10^{14}
EX $\gamma=20$	1.4	55	5.5	4.8×10^{11}

decay is measured over about three decades. Therefore an independent discriminating test is necessary. Quantum efficiency measurements provide such a test. The concentration dependence of the quantum efficiency for the various mechanisms is obtained by the integration of Eq. (13):

$$\frac{\eta_i}{\eta_0}=\frac{1}{\tau_r}\int_0^\infty \frac{I(t)}{I_0}\,dt\ . \tag{18}$$

It is interesting to note that the shapes of all the $\eta_i(C/C_0)$ curves are quite similar which can be seen in Fig. 14. The curves for the EDQ and EQQ interaction mechanisms should be between the curves for EDD and EX with $\gamma=14$, but are not shown for the sake of clarity. Putting the measured quantum efficiency η for various occupied donor concentrations C versus the C/C_0 effective concentrations obtained from fitting the decay kinetics measurements (from Table I) on a theoretical plot of $\eta(C/C_0)$ provides the desired discrimination. The best consistency as shown in Figs. 13 and 14 is obtained in our case for the exchange interaction for which the parameter γ is equal to $\gamma=14$. Figure 15 provides a correlation between the values of C/C_0 obtained from fitting the data with the exchange mechanism with $\gamma=14$ and the occupied shallow donor concentration C. This concentration was obtained from the temperature-

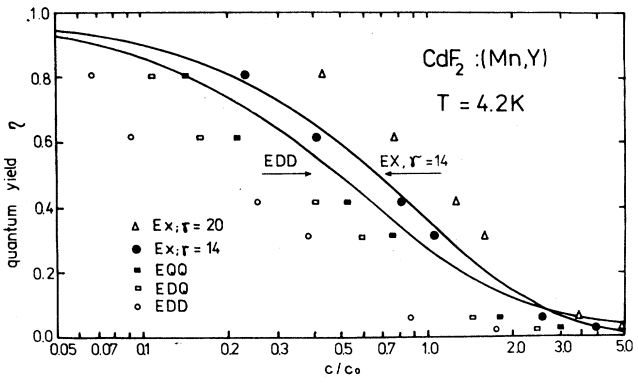

FIG. 14. Quantum efficiency correlation diagram for various energy-transfer interactions. The solid curves are predicted dependences of $\eta(C/C_0)$ for exchange (EX) with $\gamma=14$ and dipole-dipole EDD energy-transfer mechanisms.

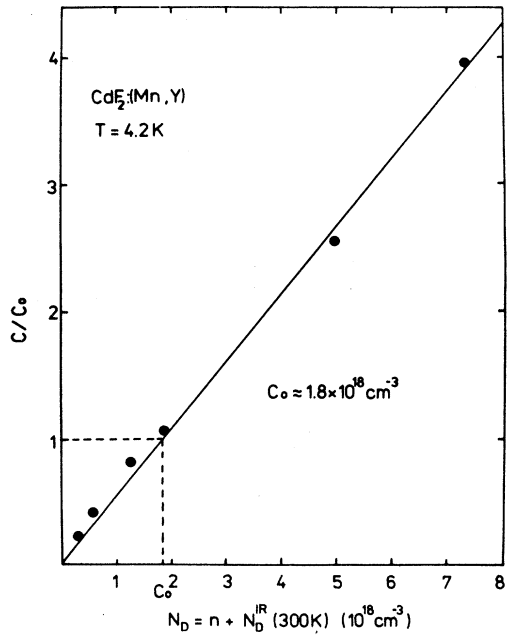

FIG. 15. The C/C_0 parameter obtained from the decay kinetics for exchange interaction with $\gamma=14$ vs the shallow donor concentration N_D.

dependent analysis of the Hall-effect carrier concentration correlated with the measurement of the shallow donor ionization absorption spectrum (Fig. 10) and employing the known photoionization cross-section callibration data[17] (see also the next section). The critical concentration C_0 obtained from this correlation equals 1.8×10^{18} cm^{-3}. Since $\gamma=2R_0/a_B$, the shallow donor Bohr radius a_B can be thus estimated. Its value of $a_B=7.3$ Å is in excellent agreement with independent estimates of this quantity from other measurements (shallow donor spectroscopy[17] or the Mott transition[22]). This agreement gives very strong support to the final conclusion on the dominant role of the exchange mechanism in this case.

B. Theoretical evaluation

The analysis of the observed kinetics of the Mn luminescence and the total quenching efficiency have led us to the conclusion that the exchange-interaction mechanism plays a dominant role in the AE. A similar conclusion can be reached analyzing the theoretical probability of the energy transfer. The EDD contribution to the energy transfer yields the power dependence of the transfer probability with a critical radius R_0(EDD) equal to[22,31]

$$R_0^6(\mathrm{EDD})=\frac{3}{64\pi^5}\frac{\lambda_0^4}{n_r^4}\sigma_{\mathrm{ion}}(\lambda_0)f\ , \tag{19}$$

where $\sigma_{\mathrm{ion}}(\lambda_0)$ is the shallow donor photoionization cross section at the maximum of the Mn^{2+} emission and f is the correction factor taking into account the spectral overlap between the Mn^{2+} emission spectrum normalized to unity $e(h\nu)$ and the shallow Y-donor photoionization absorption spectrum $a_{\mathrm{ion}}(h\nu)$:

$$f=\int_0^\infty \frac{e(h\nu)a(h\nu)}{(h\nu/h\nu_0)^4}d(h\nu)\ . \tag{20}$$

In both equations ν_0 and λ_0 refer to the maximum of the Mn^{2+} emission. In the case of CdF_2:Mn,Y this correction factor equals 3.4. The value of $\sigma_{\mathrm{ion}}(\lambda_0)$ in Eq. (20) can be taken either from the experimental results (see Fig. 10) or from the theoretical calculations of this quantity. Either of these approaches leads to a value of R_0(EDD) of about 26 Å. This value is much smaller than the value of 37 Å derived from the fit to the emission kinetics assuming validity of the EDD mechanism (see Table I). Although the discrepancy seems to be small, it is in fact large enough to rule out EDD as the dominant mechanism for the energy transfer. This is because of the 6th power of R_0 entering the AE probability [Eq. (12)]. A similar conclusion can be reached from just a simple analysis of the efficiency drop depicted in Fig. 2. For quenching larger then unity the efficiency of the Auger-quenched luminescence is given by the equation[32]

$$\frac{\eta}{\eta_0}=1-\sqrt{\pi}\exp(q^2)[1-\mathrm{erf}(q)]$$
$$=\sum_{m=1}^{\infty}(-1)^{m+1}\frac{(2m-1)!!}{(2q^2)^m}\approx\frac{1}{2q^2}\ , \tag{21}$$

where

$$q=\frac{2\pi^{3/2}}{3}N_D R_0^3\approx 3.71 N_D R_0^3 \tag{21a}$$

and

$$\mathrm{erf}(x)=\frac{2}{\sqrt{\pi}}\int_0^x \exp(-y^2)dy\ . \tag{21b}$$

To account for the 6% value of the quantum efficiency the concentration of the occupied shallow Y donors should be about 10^{21} cm^{-3} which exceeds the true value of N_D by about a factor of 100.

The higher-order multipolar contribution can also be ruled out by a similar argument. For the EDQ contribution ($m=8$) the ratio of the energy-transfer probability between EDQ and EDD is approximately given by[28] $P(\mathrm{EDQ})/P(\mathrm{EDD})\approx(a/R)^2$, where a is the Bohr radius of the shallow donor in our case. Substituting the theoretical value of R_0(EDD)=26 Å and the value of the Bohr radius $a\approx7$ Å (Ref. 17) yields the value of R_0(EDQ)$\approx$20 Å which is again much smaller than the 42 Å (see Table I) necessary to account for the observed quenching.

The only mechanism which is left is the exchange mechanism (EX). The first-principle theoretical estimate of its strength is a formidable task since it requires not only precise knowledge of the Mn wave function but also knowledge of the Bloch modulating part $u_k(\mathbf{r})$ of the wave functions of the Auger particle.[33] The problem simplifies substantially by noting that the only difference between the wave function of all centers participating in

the free-electron AE and the AE due to the weakly bound carriers is in the initial state of the energy accepting electron. In the former case it is just $u_0(\mathbf{r})$ [Eq. (5)], while in the latter it must be multiplied by the effective-mass envelope function $F(\mathbf{r})$. For the hydrogenlike donors it is a simple 1s-wave function decaying exponentially as $\exp(-r/a_B)$ with a_B being the effective Bohr radius of the shallow donor. Therefore the exchange matrix element for both cases differs only by the value of the envelope donor function $F(\mathbf{R})$ at a distance R between the shallow donor and Mn^{2+}:

$$|M_{\mathrm{EX}}^{\mathrm{bound}}(R)|^2=|F(R)|^2|M_{\mathrm{EX}}^{\mathrm{free}}|^2 . \tag{22}$$

The same relationship is obtained for the probabilities of the AE:

$$P_{\mathrm{EX}}(R)=F^2(R)C_A(\mathrm{EX}) . \tag{23}$$

Taking into account the hydrogenic shape of $F(R)$ and expressing $C_A(\mathrm{EX})$ in the same form as for the EDD case, i.e., by putting $C_A(\mathrm{EX})=[\tau_r^* n_0(\mathrm{EX})]^{-1}$, we obtain

$$P_{\mathrm{EX}}(R)=\frac{1}{\tau_r}\frac{1}{\pi a_B^3 n_0(\mathrm{EX})}e^{-2R/a_B} . \tag{24}$$

This is the exact form used in the fitting procedure above.

Since $P(R_0)=1/\tau_r$ we finally obtain

$$e-\frac{2R_0(\mathrm{EX})}{a_B}=e^{-\gamma}=\pi a_B^3 n_0(\mathrm{EX}) . \tag{25}$$

Assuming that the measured value of $n_0=2.2\times10^{15}$ cm^{-3} comes only from the EX mechanism and using the known value of $a_B=7$ Å (very close to the value of $a_B=7.3$ Å obtained from the fit of the quenching data above), we obtain the value of $\gamma=13$, which is favorably close to the value of $\gamma=14$ coming from the self-consistent fit of the kinetics and the efficiency data. This result agrees very well with the model calculations of the exchange contribution to the AE made by Majewski and Langer[33] who also concluded that even if the free-carrier AE is dominated by the EDD contribution, the bound carrier AE should be in most cases governed by the EX mechanism.

It is worth pointing out that the energy-level structure of Mn^{2+} may also favor the exchange mechanism because of its excited states have smaller total spin than the ground sextet $^6A_{1g}$. In the case of an electric-dipole mechanism, a spin-flip transition is forbidden and the contribution to the spectral transition comes from a second-order admixture of the ground sextet state with the excited quartet state via the spin-orbit interaction. In the case of the exchange-type energy transfer the total spin must be conserved, therefore the inherently low probability of the $^4T_{1g}\rightarrow{}^6A_{1g}$ spin-flip transition [τ_r (300 K)$\approx$60 ms] is not an obstacle any more since the Auger electron may simultaneously undergo a spin-flip. This peculiar energy-level structure of Mn^{2+} provides about 1000-fold enhancement factor for the EX mechanism as compared with the EDD contribution (a ratio of the spin allowed to the spin-forbidden d-d transitions in a centrosymmetric environment).

VI. SUMMARY

The experimental and theoretical results presented in this paper show that the Auger quenching of the localized-center luminescence may be the dominant nonradiative mechanism for localized defects even in weakly conducting semiconductors. The Auger effect due to free carriers should generally be stronger than that due to bound carriers. The difference between them should be diminished with the increased delocalization of the weakly bound carriers, i.e., in semiconductors characterized by a large dielectric constant and small effective mass. In our case the difference is large (about a factor of 500) due to the anomalous value of the Bohr radius of the shallow donor ($a_B\approx7$ Å).

The dominant mechanism for the AE cannot be generally predicted, since it depends on the particular energy structure of the quenched emitter, the energy to be dissipated, as well as the host band structure (possibility of a resonance condition between the quenched emission and the energetic position of the high density of states[9]). In any case the rate of the free-carrier AE must be larger than the dipole contribution, which can be estimated from Eq. (11). For most semiconductors ($\lambda_0\leq1$ μm, $n_r\leq4$) n_0 must be smaller than 10^{16} cm^{-3}. This clearly indicates the importance of the AE in quenching the emission of the localized centers in semiconductors. Quite often it has been hoped that an injection-type laser could be constructed by incorporating into the junction region of the laser diode localized impurities (especially rare-earth dopants establishing a very narrow-line emission), which could be the active center for the laser action.[34] A high probability for the AE described here makes this hope quite hard to realize, especially in the dc pumping regime.[14]

The AE can be utilized in a study of the excitation mechanism of high-field electroluminescence,[11,19,36] as well as cathodoluminescence dynamics.[11,19] It is also possible to use the AE data to estimate the cross section of the reverse process, i.e., the impact excitation of localized defects.[21]

ACKNOWLEDGMENTS

The authors wish to thank Teresa Langer and Zbigniew Kalinski for the growth and preparation of the crystals used in this study. The research has been financially supported by the Polish Academy of Sciences programs CPBP-01-04 and CPBP-01-12.

[1]A. M. Stoneham, Rep. Prog. Phys. **44**, 1251 (1979); P. T. Landsberg, Phys. Status Solidi B **41**, 457 (1970); J. M. Langer, in *Defects in Crystals,* edited by E. Mizera (World Scientific, Singapore, 1987), p. 50.

[2]L. A. Riseberg and M. J. Weber, Prog. Opt. **14**, 91 (1976); L. A. Riseberg, in *Radiationless Processes,* edited by B. Di Bartolo (Plenum, New York, 1980), p. 385; R. Reisfeld and Ch. K. Jørgensen, *Lasers and Excited States of Rare Earths* (Springer-Verlag, Berlin, 1977); R. C. Powell and G. Blasse, Struct. Bonding (Berlin) **42**, 43 (1980).

[3]M. J. Weber, Phys. Rev. B **8**, 54 (1973); H. W. Moos, J. Lumin. **1&2**, 106 (1970); R. Englman, *Non-Radiative Decay of Ions and Molecules in Solids* (North-Holland, Amsterdam, 1979).

[4]F. Auzel, in *Luminescence of Inorganic Solids,* edited by B. Di Bartolo (Plenum, New York, 1978); in *Semiconductor Optoelectronic,* edited by M. A. Herman, (Wiley, New York, 1980), p. 233.

[5]M. D. Sturge, Phys. Rev. B **8**, 6 (1973); C. H. Henry and D. V. Lang, *ibid.* **15**, 989 (1977); J. M. Langer, Rad. Eff. **72**, 55 (1983).

[6]A. Stapor and J. M. Langer, Phys. Rev. B **25**, 3407 (1982); A. Suchocki, G. D. Gilliland, and R. C. Powell, *ibid.* **35**, 5830 (1987), A. Suchocki, J. D. Allen, and R. C. Powell, *ibid.* **36**, 6729 (1987); T. Holstein, S. K. Lyo, and R. Orbach, in *Laser Spectroscopy of Solids,* edited by W. M. Yen and P. M. Selzer (Springer-Verlag, Berlin, 1981), p. 83.

[7]P. T. Landsberg and D. J. Robbins, Solid State Electron. **21**, 1289 (1978).

[8]W. Schmid, Phys. Status Solidi B **84**, 529 (1977); Solid State Electron. **21**, 1285 (1978); G. F. Neumark, D. J. DeBitetto, R. N. Bhargava, and P. M. Harnack, Phys. Rev. B **15**, 3147, 3156 (1977); K. P. Sinha and M. Di Domenico, Jr., *ibid.* **1**, 2623 (1970).

[9]N. T. Gordon and J. W. Allen, Solid State Commun. **37**, 1441 (1981).

[10]J. M. Langer and W. Walukiewicz, in *Proceedings of the X Seminar on the Physics of Semiconductors, Jaszowiec, 1980,* edited by J. M. Langer (Ossolineum, Wroclaw, 1981), p. 82; A. Suchocki, J. M. Langer, and W. Walukiewicz, in *Proceedings of the 16th International Seminar on Energy Transfer in Condensed Matter, Prague, 1981,* edited by J. Pantoflicek and W. Zachoval (Society of Czechoslovak Mathematicians and Physicists, Prague, 1981), p. 234.

[11]J. M. Langer, J. Lumin. **23**, 141 (1981).

[12]J. M. Langer, A. Suchocki, Le Van Hong, P. Ciepielewski, and W. Walukiewicz, and Physica B+C **117&118B**, 152 (1983); J. M. Langer and Le Van Hong, J. Phys. C **17**, L923 (1984).

[13]P. B. Klein, J. E. Furneaux, and R. L. Henry, Phys. Rev. B **19**, 1947 (1984); A. Zakrzewski and M. Godlewski, Phys. Rev. B **34**, 8993 (1986).

[14]J. M. Langer, in *Rare Earth Spectroscopy,* edited by B. Jeżowska-Trzebiatowska, J. Legendziewicz, and W. Strek (World Scientific, Singapore, 1985), p. 523; J. Lumin. **40&41**, 589 (1988).

[15]J. D. Kingsley and J. S. Prenner, Phys. Rev. Lett. **8**, 315 (1962); Phys. Rev. **126**, 458 (1962); P. F. Weller, Inorg. Chem. **4**, 1545 (1965); *ibid.* **5**, 736 (1966); W. Hayes, *Crystals with the Fluorite Structure* (Clarendon, Oxford, 1974).

[16]R. P. Khosla, Phys. Rev. **183**, 695 (1969).

[17]J. M. Langer, T. Langer, G. L. Pearson, B. Krukowska-Fulde, and U. Piekara, Phys. Status Solidi B **66**, 537 (1974); J. Dmochowski, J. M. Langer, Z. Kaliński, and W. Jantsch, Phys. Rev. Lett. **56**, 1735 (1986).

[18]P. J. Alonso and R. Alcala, J. Lumin. **22**, 321 (1981); A. Suchocki, Acta Physica Polonica, A **67**, 99 (1985).

[19]J. M. Langer, A. Lemańska-Bajorek, A. Suchocki, W. Walukiewicz, and B. Wiktor, J. Lumin. **24/25**, 889 (1981).

[20]T. Langer, B. Krukowska-Fulde, and J. M. Langer, Appl. Phys. Lett. **34**, 216 (1979); J. M. Langer, T. Langer, and B. Krukowska-Fulde, J. Phys. D **12**, L95 (1979).

[21]J. M. Langer, in *Semiconductor Sources of Electromagnetic Radiation,* edited by M. A. Herman (PWN–Polish Scientific, Warszawa, 1976), p. 411; in *Optoelectronic Materials and Devices,* edited by M. A. Herman (PWN–Polish Scientific, Warszawa, 1983), p. 303.

[22]M. Potemski, *Proceedings of the XI International Conference on the Physics of Semiconductors, Jaszowiec, 1981,* edited by J. M. Langer (Ossolineum, Wroclaw, 1982), p. 294.

[23]D. Hommel and J. M. Langer, J. Lumin. **18/19**, 281 (1979).

[24]B. Di Bartolo, *Optical Interaction in Solids* (Wiley, New York, 1968), p. 405.

[25]L. J. Van der Pauw, Phillips. Res. Rep. **13**, 1 (1958).

[26]V. M. Agarnovich, Usp. Fiz. Nauk. **112**, 143 (1974).

[27]Th. Forster, Ann. Phys. (Leipzig) **2**, 55 (1948); Z. Naturforsch. **4a**, 321 (1949).

[28]D. L. Dexter, J. Chem. Phys. **21**, 836 (1953).

[29]M. Inokuti and H. Hirayama, J. Chem. Phys. **43**, 1978 (1965).

[30]A. Suchocki and J. M. Langer, in *Proceedings of the XII International Conference on the Physics on Semiconductors, Jaszowiec, 1983,* edited by R. R. Gałazka and J. Rauszkiewicz (Ossolineum, Wroclaw, 1983), p. 228; in *Energy Transfer Processes in Condensed Matter,* Vol. 114 of *NATO Advanced Study Institute, Series B: Physics,* edited by B. Di Bartolo (Plenum, New York, 1984), p. 686.

[31]J. M. Langer and W. Walukiewicz, *Physics of Semiconducting Compounds,* edited by J. M. Langer (Ossolineum, Wroclaw, 1981), Vol. 2, p. 92.

[32]K. B. Eisenthal and S. Siegel, J. Chem. Phys. **41**, 652 (1964).

[33]J. A. Majewski and J. M. Langer, Acta Physica Polonica A **67**, 51 (1985).

[34]There are reports on achieving single-mode laser action on InGaAsP doped with Er (Ref. 35) although the results are ambiguous whether the intrashell transitions within the *f* erbium shell or the band-edge transitions are responsible for the lasing properties of this system.

[35]W. T. Tsang and R. A. Logan, Appl. Phys. Lett. **49**, 1686 (1986); J. P. van der Ziel, M. G. Oberg, and R. A. Logan, Appl. Phys. Lett. **50**, 1313 (1987).

[36]J. M. Langer, A. Lemanska-Bajorek, and A. Suchocki, Appl. Phys. Lett. **39**, 385 (1981).